Hyperfine-Structure Separations and Magnetic Moments of Cs^{127}, Cs^{129}, Cs^{130}, and Cs^{132}†

WILLIAM A. NIERENBERG,* HOWARD A. SHUGART, HENRY B. SILSBEE, AND R. J. SUNDERLAND‡
Radiation Laboratory and Department of Physics, University of California, Berkeley, California

(Received June 11, 1958)

The atomic hyperfine-structure separations and magnetic moments of four neutron-deficient cesium isotopes have been measured by an atomic-beam magnetic-resonance method as

Isotope	hfs, $\Delta\nu$ (Mc/sec)		Magnetic moment, μ (nm)
Cs^{127}(6.2 hr, $I=\frac{1}{2}$)	8950±200		+1.43±0.04
Cs^{129}(31 hr, $I=\frac{1}{2}$)	9200±200		+1.47±0.04
Cs^{130}(30 min, $I=1$)	6400±350	for	+1.37±0.08
	6800±350	for	−1.45±0.08
Cs^{132}(6.2 days, $I=2$)	8648±35		+2.22±0.02

The spin measurement of Cs^{132} is discussed.

INTRODUCTION

PREVIOUSLY the nuclear spins of four neutron-deficient cesium isotopes have been measured by the atomic-beam magnetic-resonance method and found to be: for 6.2-hr Cs^{127}, $I=\frac{1}{2}$; for 31-hr Cs^{129}, $I=\frac{1}{2}$; for 30-min Cs^{130}, $I=1$; and for 6.2-day Cs^{132}, $I=2$.[1,2] A brief account of the Cs^{132} spin measurement is given here. The result $I=\frac{1}{2}$ for Cs^{127} and Cs^{129} is unexpected for the odd-proton configuration of cesium, since the simple nuclear shell model would predict $I=\frac{7}{2}$ as in Cs^{133},[3] Cs^{135}, and Cs^{137},[4] or $I=\frac{5}{2}$ as in Cs^{131}.[5] This paper describes hyperfine-structure separation and magnetic-moment measurements of these four neutron-deficient cesium isotopes. The magnetic-moment measurements may aid in determining the nucleon configuration that gives rise to the observed nuclear spins.

THEORY OF THE EXPERIMENT

The work described here follows very closely that published in previous papers.[6,7] The atomic-beam apparatus using the flop-in technique[8] provides resonance indications superimposed on very low background. The focusing magnetic fields, stops, and collimators are arranged so that, except for spurious effects, no atoms reach the detector when the transition radio-frequency is off resonance. When a sensitive detector is available, resonances appear as increases in the number of atoms reaching the detector. Radioactive detection of collected activity provides a selective, sensitive, and low-background method for observing resonances of radioactive isotopes. In these experiments the cesium isotopes, deposited on sulfur collectors, are detected with thin-crystal NaI(Tl) scintillation counters by observing the K x-rays that result from electron capture and internal conversion.

All measurements are made with the cesium atoms in the $^2S_{\frac{1}{2}}$ electronic ground state. In the linear Zeeman region (at low fields) the flop-in transition frequency is given by Eq. (1). Therefore for a given magnetic field and g_J, isotopes undergo transitions at discrete frequencies which depend on the value of the nuclear spin, I:

$$\nu \cong -g_J\mu_0 H/(2I+1)h. \qquad (1)$$

The atomic hyperfine-structure separation, $\Delta\nu$, is obtained by observing the $F=I+\frac{1}{2}$, $m_F=-I-\frac{1}{2}\leftrightarrow m_F=-I+\frac{1}{2}$ transition at higher external magnetic fields. Equation (2), derived from the Breit-Rabi formula,[9] expresses the hyperfine-structure separation in terms of the transition field, H; the transition frequency, ν; and the electronic and nuclear g factors, g_J and g_I:

$$\Delta\nu=\frac{\left(\nu+\frac{g_I\mu_0H}{h}\right)\left(-\frac{g_J\mu_0H}{h}-\nu\right)}{\left[\nu+\frac{g_J\mu_0H}{(2I+1)h}+\frac{2Ig_I\mu_0H}{(2I+1)h}\right]}. \qquad (2)$$

The convention is used in which a positive magnetic moment has a positive g factor (i.e., $g_J\approx -2$). Because both $\Delta\nu$ and g_I are unknown, only two independent

† This research was supported by the U. S. Atomic Energy Commission.
* On leave as Professor in the Miller Institute for Basic Research in Science.
‡ Present address: Aerojet-General Corporation, Azusa, California.
1 Nierenberg, Shugart, Silsbee, and Sunderland, Phys. Rev. **104**, 1380 (1956).
2 Nierenberg, Hubbs, Shugart, Silsbee, and Strom, Bull. Am. Phys. Soc. Ser. II, **1**, 343 (1956).
3 H. Kopfermann, Z. Physik **73**, 437 (1932).
4 L. Davis, Phys. Rev. **76**, 435 (1949); D. E. Nagle, Phys. Rev. **76**, 847 (1949).
5 E. H. Bellamy and K. F. Smith, Phil. Mag. **44**, 33 (1953).
6 Hobson, Hubbs, Nierenberg, Silsbee, and Sunderland, Phys. Rev. **104**, 101 (1957).
7 Hubbs, Nierenberg, Shugart, Silsbee, and Sunderland, Phys. Rev. **107**, 723 (1957).
8 J. R. Zacharias, Phys. Rev. **61**, 270 (1942).
9 G. Breit and I. I. Rabi, Phys. Rev. **38**, 2082 (1931).

resonances should be necessary for a solution of Eq. (2). Because of poor resolution and the insensitivity of Eq. (2) to the g_I term, this experiment does not permit obtaining g_I and $\Delta\nu$ by simultaneous solution at two field values. However, $\Delta\nu$ and g_I are related (to within about 1%) by the Fermi-Segrè formula,[10] in which the primed quantities refer to constants of another isotope of the same element:

$$\frac{\Delta\nu}{|g_I|(2I+1)} \cong \frac{\Delta\nu'}{|g_{I'}|(2I'+1)}. \tag{3}$$

Equation (4), obtained by eliminating g_I from Eqs. (2) and (3), gives the hyperfine-structure separation provided the proper sign is chosen for the constant c_1 (the positive sign for c_1 corresponds to a positive nuclear magnetic moment):

$$\Delta\nu = 2c/[b+(b^2-4ac)^{\frac{1}{2}}], \tag{4}$$

where

$$a = [2I/(2I+1)]c_1H,$$
$$b = \nu - [1/(2I+1)]c_2H + \nu c_1H - c_1c_2H^2,$$
$$c = \nu c_2H - \nu^2,$$
$$c_1 = \pm|g_{I'}|[(2I'+1)/(2I+1)](\mu_0/\Delta\nu h),$$
$$c_2 = -g_J\mu_0/h.$$

For computational purposes the form of the quadratic formula of Eq. (4) eliminates loss of significant figures, which occurs when the more common form is used.

The hyperfine-structure separation, $\Delta\nu$, calculated for each resonance by use of Eq. (4) depends upon the choice of the sign of the magnetic moment. The sign choice that results in a consistent set of $\Delta\nu$'s is then the correct sign of the nuclear magnetic moment. The values of $\Delta\nu$ calculated with the wrong assumed sign for the magnetic moment show a smooth variation with the static transition magnetic field.

ISOTOPE PREPARATION

Cs^{127}, Cs^{129}, and Cs^{130} are produced by $I(\alpha,kn)Cs$ reactions during bombardments of BaI_2 powder with 45-Mev α particles from the Berkeley 60-inch cyclotron.[11,12] At the energies available k may be 1, 2, 3, and 4 to produce Cs^{130}, Cs^{129}, Cs^{128}, and Cs^{127}, but the Cs^{128} has too short a half-life to be treated at present. Since the cross section for a given (α,kn) reaction is a function of the α-particle energy and has a threshold below which the reaction does not occur, the production of Cs^{130} may be favored over that of Cs^{127} and Cs^{129} by degrading the α-particle energy before allowing the beam to enter the BaI_2 powder. This scheme allows the relative activity and the apparatus background of Cs^{127} and Cs^{129} to be reduced in comparison with a bombardment by full-energy α particles. The cesium activities, along with Cs^{133} carrier, are separated chemically from the target material by precipitating the target barium and resulting cerium activities with $(NH_4)_2CO_3$. After the filtrate is boiled to dryness the excess ammonium compounds are removed by decomposition and sublimation with further heating. The remaining cesium compounds are transferred to an atomic-beam oven and thoroughly dried. Before the oven is inserted into the apparatus an excess of calcium metal is added for the purpose of reducing the cesium to the atomic state by a reaction that proceeds upon heating.

Cs^{132} is produced by bombarding gaseous xenon with 12-Mev protons from the 60-inch cyclotron. The proton energy is low and only the (p,n) reaction has a usable cross section. Because there exist seven stable xenon isotopes of greater than 1% abundance, many cesium isotopes are produced. Several of these represent a small fraction of the total activity, owing to low abundance of the corresponding xenon isotope, owing to short half-life so that the isotope has decayed by the time the experiment is performed, or owing to long half-life and hence low decay rates. As a result the principal constituents of this production scheme are Cs^{129}, Cs^{131}, and Cs^{132}. Similarly xenon has been bombarded with deuterons to produce the same isotopes through (d,kn) reactions. The gas bombardment takes place in a cast aluminum container holding approximately 2 liters (STP) of xenon. The cesium activity collects on the walls of the container, since little follows the xenon when it is frozen out into a storage vessel. (Radioactive xenon isotopes are produced during deuteron bombardments, making the gas quite active.) The cesium is removed by washing the target vessel with slightly acidified water containing controlled amounts of carrier, and is then concentrated by boiling the solution almost to dryness before transferring it to the oven. Calcium is again used to reduce the cesium compounds to the atomic form.

Cs^{132} SPIN MEASUREMENT

For spin searches in the linear Zeeman region, the flop-in transition frequency is given by Eq. (1). The search is made by setting the transition frequency at the value for each spin and exposing a collector at the detector position of the apparatus. Table I gives the normalized counting rates on samples exposed at the frequencies corresponding to integral spins from 0 to 7 and half-integral spins from $\frac{1}{2}$ to 9/2. The decays of the spins $\frac{1}{2}$, 2, and $\frac{5}{2}$ are shown in Fig. 1. From the measured half-life of each sample the identities of the isotopes responsible for the signals are as follows: Cs^{129}, $I=\frac{1}{2}$; Cs^{131}, $I=\frac{5}{2}$; and Cs^{132}, $I=2$. The spurious signal on spin $\frac{3}{2}$ decayed with a half-life corresponding to that of Cs^{129} and was traced to the second harmonic content of the oscillator. The second harmonic of the $I=\frac{3}{2}$ frequency is exactly the frequency to cause $I=\frac{1}{2}$ transitions to occur. The spin measurements of this run

[10] E. Fermi and E. G. Segrè, Z. Physik **82**, 729 (1933).
[11] Fink, Reynolds, and Templeton, Phys. Rev. **77**, 614 (1950).
[12] Smith, Mitchell, and Caird, Phys. Rev. **87**, 454 (1952).

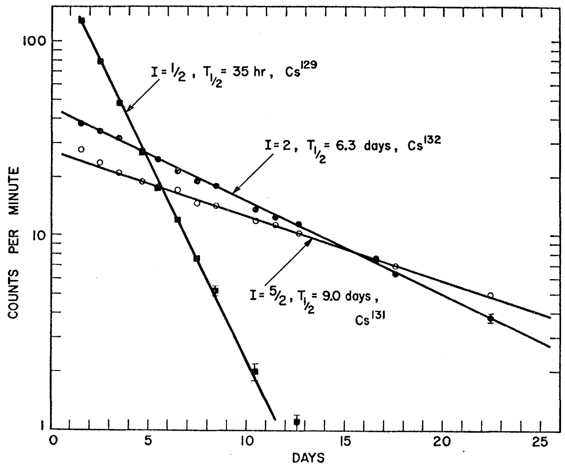

FIG. 1. Decays of the important samples from the Cs^{132} spin search. The half-life serves to identify the isotope responsible for each spin resonance.

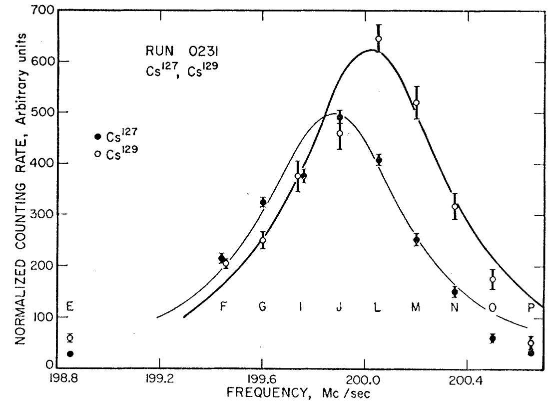

FIG. 3. A single $I=\frac{1}{2}$ resonance of Cs^{127} and Cs^{129} is decomposed into two resonances by analyzing the decay for each data point.

for Cs^{129} and Cs^{131} represent verifications of previous work using a different method of isotope preparation, and—for Cs^{131}—a different method of identification and detection.[1,5]

TREATMENT OF hfs DATA

Radioactive resonances are observed as in previous work[6,7] by counting the K x-ray activity collected on sulfur-coated buttons exposed at various settings of the transition radio-frequency. The activity on each exposure is corrected for changes in the beam intensity as measured by the height of the calibration resonance of stable Cs^{133}, which was added as carrier during the chemistry. For short-lived activities a further allowance for decay of the sample corrects the counting rates to a common time.

A symmetric resonance curve was fitted to the radioactive resonances by use of a routine programmed for the IBM 650 digital computer. Actually a parabola was fitted to the reciprocals of the counting rates by a weighted-least-squares procedure. This technique gives more weight to points near the resonance peak and decreases the effect of an asymmetric line on the determination of the peak frequency. The curve-fitting routine yields the frequencies of the resonance maximum, the resonance height, and resonance width, and the uncertainty in the peak frequency due to the statistical nature of the input data points. An example of a radioactive resonance and the fitted symmetric curve is shown in Fig. 2.

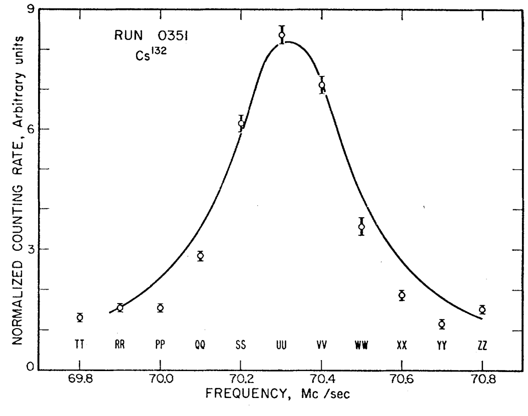

FIG. 2. A resonance of Cs^{132} at 70 Mc/sec showing the symmetric curve fitted to the data points.

Because the Cs^{127} and Cs^{129} resonances are not resolved at the highest fields used, it is necessary to allow each resonance point to decay to obtain an indication of the isotopic composition of that point. In this way it is possible to decompose the resonance into two component resonances. For this purpose the known half-lives are used to fit the amplitudes of the component isotopes from the decay curve. The fit is done by a least-squares technique using digital computer facilities. Figure 3 shows the results of a decomposition of one of the high-field Cs^{127} and Cs^{129} resonances.

The hyperfine-structure separation is calculated by use of the peak frequency of the radioactive resonance and the value of the transition magnetic field as given

TABLE I. Counting rates for Cs^{132} spin search.

Spin	Counting rate (arbitrary units)	Isotope identity
0	4.8 ± 0.4	
$\frac{1}{2}$	127.8 ± 1.8	Cs^{129}
1	6.1 ± 0.4	
$\frac{3}{2}$	35.7 ± 1.0^{a}	Cs^{129a}
2	54.5 ± 1.2	Cs^{132}
$\frac{5}{2}$	27.7 ± 0.9	Cs^{131}
3	4.8 ± 0.4	
$\frac{7}{2}$	5.0 ± 0.4	
4	6.5 ± 0.4	
9/2	4.5 ± 0.4	
5	7.5 ± 0.4	
6	3.8 ± 0.3	
7	2.7 ± 0.3	

[a] The second harmonic of the 3/2 frequency caused a resonance of $I=\frac{1}{2}$ to appear on this sample.

by the Cs^{133} resonance at the time the radioactive peak exposures were taken. The constants used in the calculations are as follows:

$$Cs^{133}: \quad I=\tfrac{7}{2}, \quad g_J=-2.00250\pm0.00006,^{13}$$
$$\Delta\nu=9192.63183\pm0.00001 \text{ Mc/sec},^{14}$$
$$\mu_I=+2.57887\pm0.00030 \text{ nm},^{15}$$
$$\mu_0=(0.92732\pm0.00006)\times10^{-20} \text{ erg/gauss},^{16}$$
$$h=(6.6252\pm0.0005)\times10^{-27} \text{ erg-sec},^{16}$$
$$M/m=1836.13\pm0.04.^{16}$$

The error placed on the calculated hyperfine-structure separations comes from the uncertainty in calibrating

TABLE II. Summary of calculations of hyperfine-structure separation.

Cs^{133} resonance frequency (Mc/sec)	Radioactive resonance frequency (Mc/sec)	hfs (assumed positive moment) (Mc/sec)	hfs (assumed negative moment) (Mc/sec)
Cs^{127}, Cs^{129} unresolved[a]			
32.195±0.010	127.283±0.289	10 400±1900	12 400±3200
32.171±0.010	127.269±0.165	9900±1000	11 600±1600
32.225±0.015	127.262±0.283	11 400±2200	14 200±4200
Cs^{127}			
50.787±0.010	200.016±0.089	8950±200	9630±240
50.811±0.010	200.104±0.067	8960±160	9640±190
	Weighted average	8950±200	
Cs^{129}			
50.787±0.010	199.873±0.084	9245±200	10 000±250
50.811±0.010	200.019±0.077	9130±180	9860±230
82.005±0.020	319.314±0.217	9310±200	9760±230
	Weighted average	9200±200	
Cs^{130}			
18.026±0.010	48.293±0.141	5430±880	5850±1100
34.106±0.010	91.124±0.150	6610±400	7000±480
34.070±0.018	91.096±0.103	6430±280	6790±330
	Weighted averages	6400±350	6800±350
Cs^{132}			
21.296±0.010	34.000±0.075	9700±1400	12 400±3000
43.964±0.010	70.318±0.059	8520±220	9180±270
81.399±0.010	129.989±0.046	8651±55	8999±61
126.039±0.010	200.988±0.072	8650±35	8864±38
	Weighted average	8648±35	

[a] Values not used in weighted averages.

the magnetic field, and from the uncertainty in placing the peak frequency of the radioactive resonance. The field-calibration resonance uncertainty is estimated as the possible error from considerations of settability, consistency, and drift. For the uncertainty in the radioactive resonance, the computer routine furnished information about the width of the resonance and the uncertainty in the peak frequency due to the statistical uncertainties of the input resonance points. The final error in the radioactive-resonance-peak frequency is

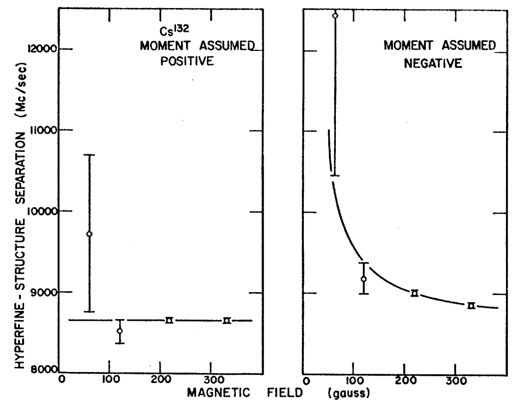

FIG. 4. Variation of the measured hyperfine-structure separation of Cs^{132} with external magnetic field when the magnetic moment is chosen first positive and then negative. The consistency of the values for the positive assumption establishes a positive magnetic moment for this isotope.

obtained by combining the statistical uncertainty of the resonance peak with one-eighth of the frequency width at half-maximum. The results of these calculations appear in Table II. For the sign determination (Figs. 4 and 5) the errors are calculated as described above except that an uncertainty of one-twentieth of the width at half-maximum is used.

RESULTS

The final weighted averages for the hyperfine-structure separations are shown in Table III. The stated error of the final value is taken as the error of the highest field measurement. The errors in the stated magnetic moments are due to the errors in the hyperfine-structure separations. No correction for diamagnetic shielding have been applied to the magnetic-moment values in Table III.

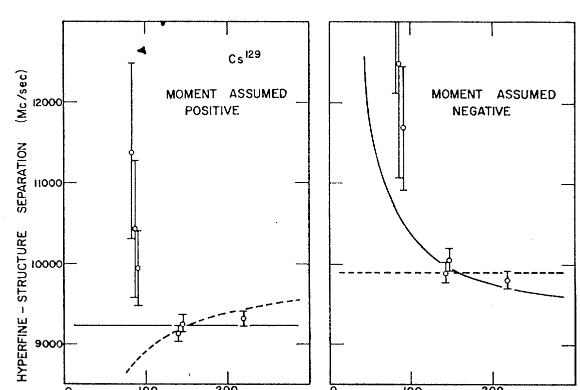

FIG. 5. Variation of the measured hyperfine-structure separation of Cs^{129} with external magnetic field. The predicted values of the experimental data for positive- and negative-magnetic-moment assumptions are shown by the solid curve and dashed curve, respectively.

[13] Brix, Eisinger, Lew, and Wessel, Phys. Rev. 92, 647 (1953).
[14] L. Essen and J. V. L. Parry, Nature 176, 280 (1955).
[15] Harold E. Walchli, Oak Ridge National Laboratory Report ORNL-1469, Supplement II, February, 1955 (unpublished).
[16] J. W. M. DuMond and E. R. Cohen, Revs. Modern Phys. 25, 706 (1953).

TABLE III. Summary of results.

Isotope	$T_{\frac{1}{2}}$	Spin	hfs, $\Delta\nu$ (Mc/sec)		Magnetic moment, μ (nm)
Cs^{127}	6.2 hr	$\frac{1}{2}$	8950 ± 200		$+1.43\pm0.04$
Cs^{129}	31 hr	$\frac{1}{2}$	9200 ± 200		$+1.47\pm0.04$
Cs^{130}	30 min	1	6400 ± 350	for	$+1.37\pm0.08$
			6800 ± 350	for	-1.45 ± 0.08
Cs^{132}	6.2 days	2	8648 ± 35		$+2.22\pm0.02$

Sign determinations are made by inspection of Figs. 4 and 5, in which the $\Delta\nu$ values are plotted as a function of magnetic field for an assumed positive moment and for an assumed negative moment. The errors shown in these figures are smaller than those of Table II, as discussed earlier. From consistency of the values for the assumed positive moment in Fig. 4, Cs^{132} is clearly assigned a positive magnetic moment. The evidence for the sign of the moment of Cs^{127} and Cs^{129} is less definite. Figure 5 shows that a positive-moment assumption for Cs^{129} is slightly more consistent with the data than a negative-moment assumption. On this basis a positive sign for the magnetic moment of Cs^{127} and Cs^{129} is chosen. Insufficient data on Cs^{130} make it impossible at present to determine the sign of its magnetic moment.

DISCUSSION

With these measurements a series of ten cesium isotopes has been investigated by atomic-beam methods. Of special interest, the series Cs^{137},[17] Cs^{135},[17] Cs^{133},[17] Cs^{131},[5] Cs^{129}, and Cs^{127} represent neutron configurations extending away from a closed shell of 82 neutrons[18] in Cs^{137}. The spin of $\frac{7}{2}$ for Cs^{137}, Cs^{135}, and Cs^{133} is in agreement[18] with the simple single-particle shell model which assumes that the odd proton moves in a spherical potential associated with closed shells of nucleons. While the $\frac{5}{2}$ spin of Cs^{131} is not difficult to explain with the shell model, the $\frac{1}{2}$ spins of Cs^{127} and Cs^{129} would require reordering many of the levels in the 55th-proton region. Nuclear spectroscopic investigations of Cs^{127} and Cs^{129} have led to an incorrect assignment of $\frac{5}{2}$ for the probable spin of these nuclei.[19,20]

The magnetic moments of Cs^{127} and Cs^{129} lie approximately midway between the Schmidt limits and are about 10% smaller than those due to the $s_{\frac{1}{2}}$ proton of Tl^{203} and Tl^{205}. Thus the magnetic moments agree well with that of an $s_{\frac{1}{2}}$ proton, and the large deviation from the Schmidt limits is explained by configuration mixing.[21,22] However, the occurrence of an $s_{\frac{1}{2}}$ assignment for the 55th proton is difficult to imagine on the basis of the existing single-particle shell model, but may become apparent with a more complete model. Also, with the simple j-j coupling scheme, it is not possible to couple particles in $j=\frac{7}{2}$ or $j=\frac{5}{2}$ levels to give a resultant spin of $\frac{1}{2}$.

Another approach to explaining the spin and moment results rests with the unified model in which the odd particles move in a deformed potential.[23–26] Some of the degeneracy of the single-particle shell model is removed and a quantum number that represents the component of the single-particle angular momentum on the nuclear axis of symmetry becomes important. The relative spacing of levels depends on the degree of core deformation.[25] Although this model is known to work best in regions quite distant from closed shells, it has been applied here to the Cs^{127} and Cs^{129} nuclei where the configuration consists of 5 particles over the 50-proton shell and 8 to 10 neutrons below the 82-neutron shell. Preliminary calculations by Uretsky have shown that equilibrium deformations having spin $\frac{1}{2}$ may be obtained from the unified model in two ways.[27] According to the notation of Mottelson and Nilsson,[26] spin $\frac{1}{2}$ occurs for 55 protons from level No. 34, deformation parameter $\eta\cong+3$ (prolate), with $\mu=+2.0$ nm, and from level No. 30, $\eta\cong-4$ (oblate), with $\mu=+1.4$ nm. The latter magnetic moment agrees well with the measured values, while the former is about 45% larger than the experimental value. Although 55 protons represent the region where the quadrupole moment is changing from negative to positive with the addition of protons, it is likely that the intrinsic deformation of the Cs^{127} and Cs^{129} ($I=\frac{1}{2}$) nuclei is oblate. Unfortunately, owing to the lack of an observable quadrupole moment for a spin-$\frac{1}{2}$ nucleus, a measurement of the intrinsic deformation is quite difficult. As a result this independent check on the collective model is unavailable.

ACKNOWLEDGMENTS

The authors wish to thank Dr. Jack L. Uretsky for permission to include the results of his unified-model calculations in the discussion. The assistance of Mr. W. Bruce Ewbank during the later parts of this work is gratefully acknowledged.

[17] Stroke, Jaccarino, Edmonds, and Weiss, Phys. Rev. **105**, 590 (1957).

[18] M. G. Mayer and J. Hans D. Jensen, *Elementary Theory of Nuclear Shell Structure* (John Wiley and Sons, Inc., New York, 1955).

[19] A. H. Wapstra, Physica **19**, 671 (1953).

[20] G. J. Nijgh, thesis, (Drukkerij Wed. G. Van Soest., Amsterdam, 1955).

[21] R. J. Blin-Stoyle, Proc. Phys. Soc. (London) **A66**, 1158 (1953).

[22] A. Arima and H. Horie, Progr. Theoret. Phys. (Japan) **12**, 623 (1954).

[23] A. Bohr, Phys. Rev. **81**, 134 (1951).

[24] A. Bohr and B. R. Mottelson, Kgl. Danske Videnskab. Selskab, Mat.-fys. Medd. **27**, 16 (1953).

[25] S. G. Nilsson, Kgl. Danske Videnskab. Selskab, Mat.-fys. Medd. **29**, 16 (1955).

[26] B. R. Mottelson and S. G. Nilsson, Phys. Rev. **99**, 1615 (1955).

[27] Jack L. Uretsky, University of California Radiation Laboratory (private communication).